# Stopping and manipulating light using a short array of active microresonators

Yannick Dumeige

# Stopping and manipulating light using a short array of active microresonators

Y. Dumeige[(a)]

*ENSSAT-FOTON (CNRS-UMR 6082)/Université de Rennes 1 - 6 rue de Kerampont, Boîte Postale 80518, 22300 Lannion, France, EU*

PACS 42.60.Da – Resonators, cavities, amplifiers, arrays, and rings
PACS 42.25.Bs – Wave propagation, transmission and absorption
PACS 42.65.Re – Ultrafast processes; optical pulse generation and pulse compression

**Abstract –** We theoretically propose a light-stopping process that uses loss and gain dynamical tuning in short coupled-resonator delay lines. The structure is made of four resonators and is optimized to avoid pulse distortion in the passive regime. The loss and gain modulations allow the resonant structure to be isolated from the access waveguide and the pulse to be stored. We demonstrate via numerical simulations the pulse storing process and show that this active delay line also induces nonlinear effects leading to pulse compression. This last property could be useful for pulse dispersion tailoring.

**Introduction.** – The possibility of slowing down or storing light holds great interests in classical or quantum optical communications [1,2]. In this context, integrated optical delay lines or buffers are key elements for more complex system of optical signal processing. In the purpose to miniaturize the device, different schemes have been proposed using electronic or photonic resonances. Among them, microresonator-based devices seem to provide a potential photonic circuit platform for this purpose [3]. Nevertheless, resonant photonic structure performances are intrinsically limited by the delay-bandwidth product which states that the delay produced by the resonant process is inversely proportional to the resonance bandwidth [4]. Consequently, for a given pulse duration the maximal distortion-free delay is fixed. To overcome this strong limitation, some strategies have been proposed and demonstrated. One first approach consists in designing complex artificial photonic media such as photonic crystal structures or coupled resonator-based waveguides in order to flatten their group velocity dispersion [4–7]. The recently proposed dynamical control of the optical properties of resonant structures which allows light-stopping is a powerful alternative [8–17]. This process relies on a photonic structure with an initial state possessing a large bandwidth allowing the incident pulse to be briefly stored [18]. After the pulse has *entirely* entered the structure, its group velocity is adiabatically decreased. The pulse spectrum is strongly compressed, which allows to stop it without distortion [19]. If the process is reversible, the pulse can be released in principle after an arbitrarily long delay. This light-stopping scheme has been studied in Bragg or coupled microresonator periodical structures [9,12,13,16]. From another point of view, it has been shown that the use of arrays of active microresonators or lasers can be used to constitute almost lossless delay lines [20–24]. In this paper, we propose to use a short array of four active coupled microresonators instead of a long chain of microresonators. This structure is used as an all pass filter (APF) whose gain or optical losses can be dynamically tuned. By using a particular coupling scheme, the gain or loss changes will also modify the coupling of the resonators with the access line. We will show as an example whose parameters are compatible with III-V semiconductor technology, that light-stopping is possible using such a very compact structure and that it could also be used for tunable dispersion compensation or pulse compression.

**Single microresonator APF.** – In order to introduce and to highlight the interest of using active coupled microresonators, we start with a short review of the single microresonator APF [4] properties which is also the building block constituting the coupled structure. Thus we consider the simplest structure that consists of a single

[(a)]E-mail: yannick.dumeige@enssat.fr; yannick.dumeige@univ-rennes1.fr

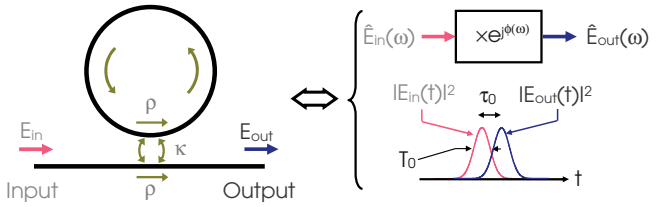


Fig. 1: (Colour on-line) Single microresonator APF side coupled to a bus waveguide. The APF induces a phase shift $\phi(\omega)$ in an input field $\hat{E}_{\rm in}(\omega)$ and introduces a group delay $\tau_0 = \tau_{\rm g}(0)$ on an optical pulse $E_{\rm in}(t)$ of duration $T_0$. The delayed pulse is noted $E_{\rm out}(t)$.

microring resonator made of a nondispersive material with refractive index $n$. The ring perimeter is $L = 2\pi R$ and its angular resonant frequency is noted $\omega_0 = 2\pi c M_0/(nL)$ (where $M_0$ is a positive integer). The resonator is side coupled to an access waveguide with an amplitude coupling coefficient $\kappa$ (related to $\rho$ by $\kappa^2 + \rho^2 = 1$). If we note the input and output fields, respectively, $E_{\rm in}(t)e^{-j\omega_0 t}$ and $E_{\rm out}(t)e^{-j\omega_0 t}$ and their corresponding inverse Fourier transforms $\hat{E}_{\rm in}(\omega)$ and $\hat{E}_{\rm out}(\omega)$, we have

$$E_{\rm out}(t) = \int_{-\infty}^{+\infty} \hat{E}_{\rm out}(\omega) e^{-j(\omega-\omega_0)t}\,{\rm d}\omega. \qquad (1)$$

The transfer function of the APF filter $t = \sqrt{T}e^{j\phi}$ is defined as

$$t(\omega) = \frac{\hat{E}_{\rm out}(\omega)}{\hat{E}_{\rm in}(\omega)} = \frac{\rho - ae^{j\varphi}}{1 - \rho a e^{j\varphi}}, \qquad (2)$$

where $\varphi = n\omega L/c = \omega\tau_L$ is the one-round-trip accumulated phase, $\tau_L$ is the round-trip duration, and $a$ is the round-trip amplitude attenuation. In the aim of optical function integration, we assume a highly resonant structure, consequently $\rho \approx 1$ (here $\rho$ is a positive real number). If we consider the particular case of a lossless resonator ($a = 1$), we obtain $T(\omega) = |t(\omega)| = 1$, and thus the device only introduces a frequency-dependent phase shift:

$$\phi(\omega) = \pi + \varphi + 2\arctan\frac{\rho\,\sin\varphi}{1 - \rho\,\cos\varphi}, \qquad (3)$$

which can be expanded around $\omega_0$:

$$\phi(\omega) = \pi + \tau_0 \cdot (\omega - \omega_0) + \sum_{p=2}^{+\infty} \frac{\beta_p(\omega_0)}{p!}(\omega - \omega_0)^p\ (2\pi), \qquad (4)$$

where $\tau_0 = \tau_{\rm g}(\omega_0) \approx 2\tau_L/(1-\rho)$ is the group delay introduced at resonance by the filter calculated using

$$\tau_{\rm g}(\omega) = \frac{\partial\phi}{\partial\omega} = \tau_L \frac{1-\rho^2}{1+\rho^2-2\rho\,\cos\varphi}; \qquad (5)$$

$\beta_p = \partial^p\phi/\partial\omega^p$ for $p \geqslant 2$ are the higher dispersion orders. Note that for the simple APF represented in fig. 1, the even dispersion orders vanish since $\tau_{\rm g}(\omega)$ is a periodic even

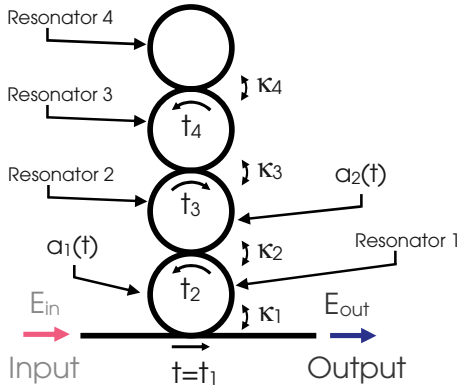


Fig. 2: (Colour on-line) Chain of active and passive microresonators. The round-trip attenuations $a_1$ and $a_2$ of resonators 1 and 2 can be dynamically tuned. The two other resonators are passive and their round-trip attenuation is kept equal to 1.

function. Neglecting these high-order dispersion terms, the output field can be written as

$$E_{\rm out}(t) = -\int_{-\infty}^{+\infty} \hat{E}_{\rm in}(\omega) e^{-j(\omega-\omega_0)(t-\tau_0)}\,{\rm d}\omega. \qquad (6)$$

Consequently, $|E_{\rm out}(t)|^2 = |E_{\rm in}(t-\tau_0)|^2$ and the input field is delayed without distortion by an amount $\tau_0$. This is not valid for an incident field as a short pulse, whose bandwidth is comparable to the full width at half-maximum (FWHM), $\Delta\nu \approx (1-\rho)/(\pi\tau_L)$: in this case, the third-order dispersion $\beta_3(\omega_0)$ is no longer negligible which leads to a strong distortion of the pulse. Thus in the case of the single microring APF, for a given pulse bandwidth, the maximal delay without too strong distortion is given by the delay-bandwidth product: $\tau_0\Delta\nu = 2/\pi \approx 0.64$. In the case of a Gaussian input pulse of temporal width $T_0$ centered at $t_{\rm c}$: $E_{\rm in}(t) = E_0 e^{-2\ln 2(t-t_{\rm c})^2/T_0^2}$, the fractional delay FD is given by $\tau_0/T_0 = 1/\ln 2 \approx 1.44$. As already noticed in the Introduction, this feature strongly limits the use of single passive microresonators to buffer optical bits. Moreover, since the delay is shorter than the whole duration of the pulse, the pulse cannot be stored entirely in the resonator, and the single resonator APF should not be used for the all-optical light-stopping process.

**Light-stopping process.** – It is possible to increase the device bandwidth in comparison with the single resonator APF, and thus to improve the fractional delay by coupling several lossless microresonators [5,6]. This will be the starting point of our dynamic light-stopping process which requires an initial state with a large bandwidth allowing to temporarily store the incident pulse. The proposed structure is shown in fig. 2. It consists of a unidimensional array of four identical single mode microrings of radius $R \approx 9.67\,\mu$m and effective index $n = 2.5$ whose common resonant wavelength is $\lambda_0 = 1.55\,\mu$m as represented in fig. 2. The coupling coefficient between resonators $i$ and $i-1$ for $i \in \{2,3,4\}$ is $\kappa_i$. $\rho_i$ defined by

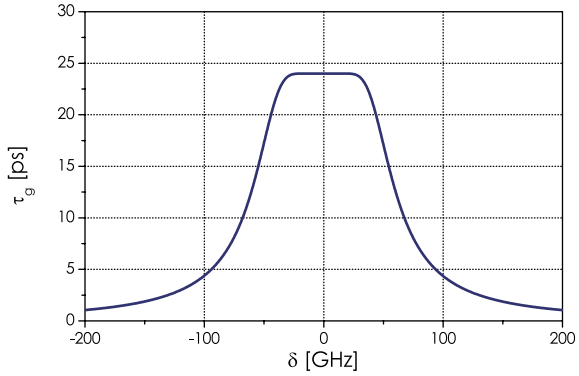


Fig. 3: (Colour on-line) Group delay introduced by the microresonator array as a function of frequency in the initial state. Note that in this case the structure is perfectly transparent: $\alpha_i = 0$ for $i \in \{1, 2, 3, 4\}$.

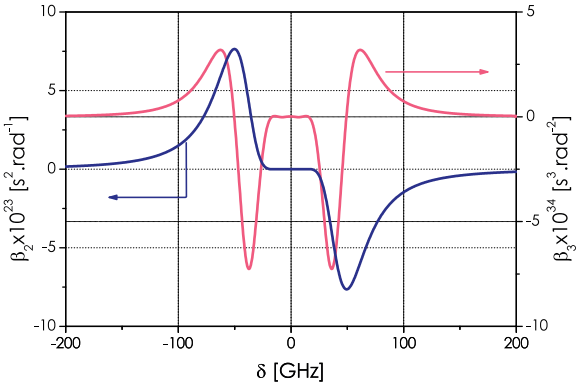


Fig. 4: (Colour on-line) Group delay dispersion $\beta_2$ and third-order dispersion $\beta_3$ of the microresonators array in the initial state ($\alpha_i = 0$ for $i \in \{1, 2, 3, 4\}$).

$\rho_i^2 + \kappa_i^2 = 1$ is assumed real and positive. Similarly, the coupling coefficient between the bus waveguide and the first resonator is $\kappa_1$. The amplitude transfer function of the unit cell is $t = \sqrt{T}e^{j\phi} = t_1$, where we calculate $t_1$ by the recursive relation using eq. (2) [25]:

$$t_i = \frac{\rho_i - t_{i+1} a_i e^{j\varphi}}{1 - t_{i+1}\rho_i a_i e^{j\varphi}}. \tag{7}$$

Here the round-trip amplitude attenuation in loop $i$, $a_i$, is related to the intensity loss coefficient $\alpha_i$ by $a_i = \exp(\alpha_i \pi R)$ and $\varphi$ still represents the round-trip phase shift which is the same in the four resonators. In the initial state all the resonators are lossless, thus $\alpha_i = 0$ for $i \in \{1, 2, 3, 4\}$. Different ways such as circuit-based methods [26] can be adopted to cancel the third-order dispersion and to increase the bandwidth of the device by optimizing the coupling coefficient values. Here we used a numerical optimization to calculate the coupling coefficients $\mathbf{k} = (\kappa_1, \kappa_2, \kappa_3, \kappa_4)$ of the structure. The objective function $\varepsilon$ is defined by

$$\varepsilon(\mathbf{k}) = \sum_{\delta \in I} \left[\tau_0 - \tau_g(\delta, \mathbf{k})\right]^2, \tag{8}$$

where $\tau_0$ is the targeted delay over a bandwidth $B$, then $I = [-B/2, B/2]$. By minimizing $\varepsilon$ we obtain a flat group delay for a bandwidth $B$ which also leads to the cancellation of $\beta_3(0)$. In the next section we will use $T_0 = 10\,\text{ps}$ long Fourier transform pulses for the time domain simulations. The bandwidth of such pulses is approximately $B = 40\,\text{GHz}$: in this case, the optimization scheme gives $\mathbf{k} = j(0.740, 0.233, 0.113, 0.074)$. The group delay and $\beta_p(\delta)$ for $p = \{2, 3\}$ are given in figs. 3 and 4, respectively, where we define the frequency detuning $\delta$ by $\omega = \omega_0 + 2\pi\delta$. The maximal delay is $\tau_0 = 24\,\text{ps}$ and the group delay bandwidth is $\Delta\nu = 120\,\text{GHz}$. The simultaneous cancellations of $\beta_2(0)$ and $\beta_3(0)$ lead to an increase of the delay-bandwidth product up to 2.88. For a 10 ps long Gaussian pulse,

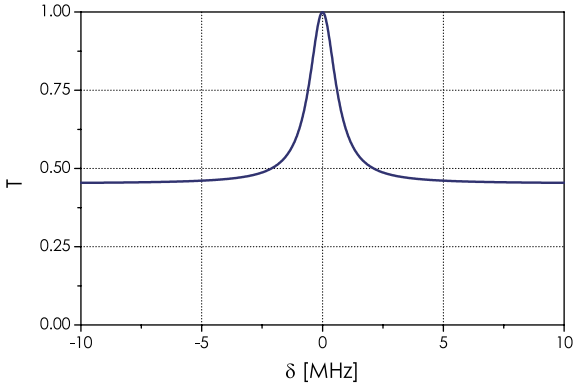


Fig. 5: (Colour on-line) Transmission of the whole structure after dynamical tuning ($\alpha_1 = -3.12 \times 10^3\,\text{cm}^{-1}$, $\alpha_2 = 9.15\,\text{cm}^{-1}$, and $\alpha_3 = \alpha_4 = 0$).

the delay bandwidth $\Delta\nu$ is about three times the pulse bandwidth, and the FD is equal to 2.4. Consequently, the proposed structure can be used to temporarily store such a short 10 ps pulse. When the pulse has completely entered the structure, the field is localized into resonators 2 and 4. By adiabatically decreasing $a_1$, it is possible to insulate resonators 2, 3, and 4 from the bus waveguide. During this time, $a_2$ is slightly increased in order to compensate for the optical losses due to the coupling with resonator 1. This scheme allows the pulse to be stored inside resonators 2, 3, and 4. To achieve this, we assume very high losses in resonator 1 $\alpha_1 = -3.12 \times 10^3\,\text{cm}^{-1}$ and a small gain in resonator 2 $\alpha_2 = -\ln\rho_2/(\pi R) = 9.15\,\text{cm}^{-1}$ used to compensate for the losses induced by resonator 1. Figures 5 and 6 represent the transmission of the structure and the associated group delay after the dynamical tuning of $\alpha_1$ and $\alpha_2$: i) The transmission remains equal to 1 at resonance which insures that the process is lossless; ii) the bandwidth is drastically reduced to few MHz which will lead to a pulse spectrum compression [9]; and iii) the group delay has been increased by more than 3 orders of magnitude, and thus the pulse can be stored for a very long time inside the resonator chain.

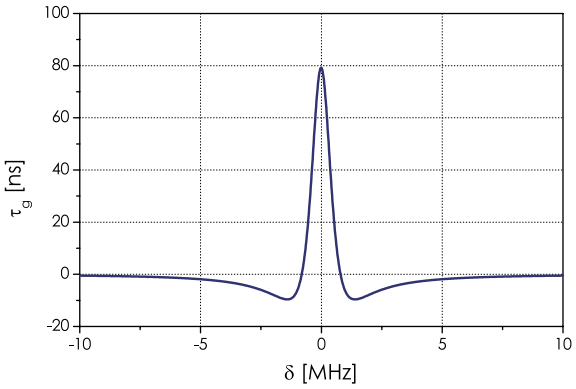


Fig. 6: (Colour on-line) Group delay introduced by the whole structure after dynamical ($\alpha_1 = -3.12 \times 10^3\,\mathrm{cm}^{-1}$, $\alpha_2 = 9.15\,\mathrm{cm}^{-1}$, and $\alpha_3 = \alpha_4 = 0$).

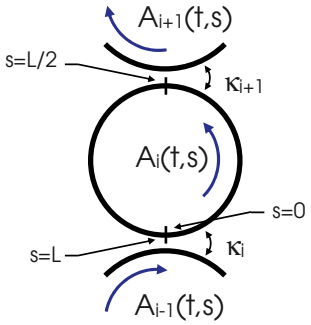


Fig. 7: (Colour on-line) Coupling scheme using in the time domain simulations. $A_i(t,s)$ is the field envelope in the ring $i$ at the curvilinear abscissa $s$.

**Time domain simulations.** – We have checked both the light-stopping process and the pulse releasing from the device using the coupled mode theory in the time domain [12,13,27,28]. The time variations of the field envelope $A_i(t,s)$ (where $s$ is the curvilinear abscissa as defined in fig. 7) in each half-microresonator is given by

$$A_i(s, t+\delta t) = A_i(s-\delta s, t) e^{j\eta_i(t)\delta s}, \tag{9}$$

where $\eta_i(t) = n\omega_0/c - j\alpha_i(t)/2$. This finite difference formulation of the wave equation slowly varying envelope approximation is valid under the assumption of a non-dispersive material. Thus, we implicitly consider that the pulse propagates with a group velocity equal to the phase velocity and that the group velocity dispersion (GVD) is negligible. This assumption is often relevant for coupled resonator structures since their structural dispersion is several orders of magnitude higher than the material dispersion [27,28]. The time and space steps are related by $\delta t = n\delta s/c$ with $\delta s \approx 1.6\,\mu$m. For the microring $i$, the coupling between the other resonators (see fig. 7) is taken into account in $s = 0$ for $i \in \{2,3,4\}$ by

$$A_i(0^+, t) = \rho_i A_i(L^-, t) + j\kappa_i A_{i-1}(\ell^-, t) \tag{10}$$

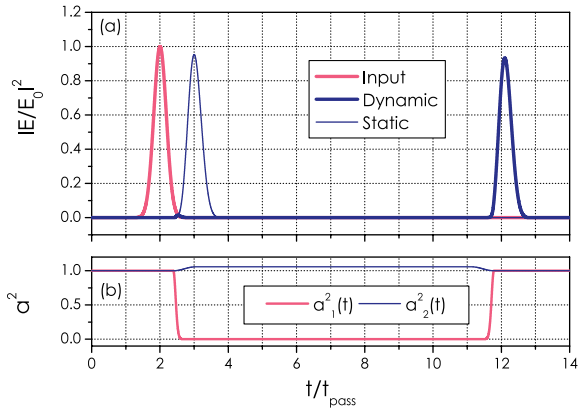


Fig. 8: (Colour on-line) Light-stopping process simulation in the time domain. (a) Input and output pulses when resonator properties are dynamically tuned (noted dynamic). We also represented the output pulse without adiabatic tuning (noted static). (b) Temporal variations of the optical losses in the first resonator and optical gain in the second resonator. The storing duration is $\Delta t = 8.1 t_{\mathrm{pass}}$.

and in $s = \ell = L/2$ for $i \in \{1,2,3\}$ by

$$A_i(\ell^+, t) = \rho_{i+1} A_i(\ell^-, t) + j\kappa_{i+1} A_{i+1}(L^-, t). \tag{11}$$

The injection of the input field and the calculation of the output field are carried out using:

$$\begin{cases} A_1(0^+, t) &= \rho_1 A_1(L^-, t) + j\kappa_1 E_{\mathrm{in}}(t), \\ E_{\mathrm{out}}(t) &= \rho_1 E_{\mathrm{in}}(t) + j\kappa_1 A_1(L^-, t). \end{cases} \tag{12}$$

Using this integration scheme and the coupling coefficients, we simulated the propagation of a $T_0 = 10\,$ps long input Gaussian pulse. As represented in fig. 8(a) in thin line, without active modulation of the losses or gain in resonators 1 and 2, the pulse is delayed by $t_{\mathrm{pass}} = 23.2\,\mathrm{ps} \approx \tau_0$ in good agreement with the stationary calculations. Note that the key point is that this static delay (noted $t_{\mathrm{pass}}$) is much longer than the pulse duration which allows the pulse to be temporarily stored inside the structure. Now we describe the light-stopping process that we propose. When the pulse completely entered the structure ($t \approx 2.4 t_{\mathrm{pass}}$), we started to modulate adiabatically $\alpha_1$ and $\alpha_2$ as it is shown in fig. 8(b). This dynamic tuning lasts 15 ps. At $t \approx 3 t_{\mathrm{pass}}$, the pulse is stored inside resonators 2, 3, and 4. At $t = 11.1 t_{\mathrm{pass}}$, we start to reverse the loss/gain modulation and the stored pulse is released from the system at $t = 12.1 t_{\mathrm{pass}}$. Figure 9 represents the temporal profile of the input and the output pulses in the static and dynamic configurations. Even in the static case, the pulse is slightly distorted since it is very short. It would be possible to reduce this residual distortion by adding more resonators, but in this work we want to reduce the number of resonators to the minimum. Nevertheless, the dynamic process has not induced much distortion. It is crucial to note that in the presented example the storing duration ($\Delta t = 8.1 t_{\mathrm{pass}} \approx 188\,\mathrm{ps}$) has been chosen in

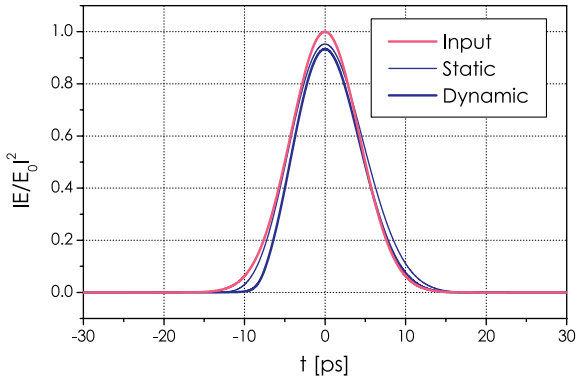


Fig. 9: (Colour on-line) Temporal profile comparison between the input $|E_{\rm in}/E_0|^2$ and the output $|E_{\rm out}/E_0|^2$ pulses in the static and dynamic cases for a storing duration $\Delta t = 8.1 t_{\rm pass}$.

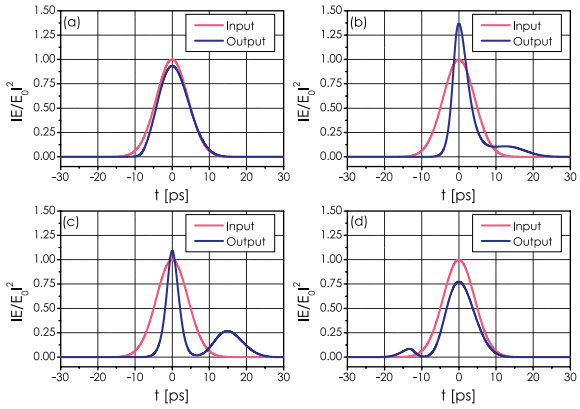


Fig. 10: (Colour on-line) Temporal profile comparison between the input $|E_{\rm in}/E_0|^2$ and the output pulses $|E_{\rm out}/E_0|^2$ in the dynamic case for different values of storing duration (a) $\Delta t = 4.04 t_{\rm pass}$, (b) $\Delta t = 3.35 t_{\rm pass}$, (c) $\Delta t = 3.49 t_{\rm pass}$, and (d) $\Delta t = 3.78 t_{\rm pass}$.

order to minimize the pulse distortion. Other simulations have shown that by increasing or decreasing the storing time, the pulse periodically recovers its Gaussian shape. This period is about a multiple of $t_{\rm pass}$. Between two optimal values of the storing time, the pulse is strongly distorted. This is illustrated by the results obtained for different storing durations presented in fig. 10: (a) in this example, the storing duration is half the previous one and the pulse profile remains almost Gaussian (the tolerance in the storing duration here is about $0.23 t_{\rm pass} \approx 5.3\,$ps); (b) the pulse can be compressed due to the combination of the dispersive properties of the delay line and the nonlinear effects induced by the dynamic tuning process [17,29]; (c) and (d) depending on the value of the storing duration the effective dispersion properties of the structure can be opposite. The interest of this effect is that in this configuration, the nonlinear pulse compression does not depend on the power of the pulse as is the case in pulse compression based on the optical Kerr effect. Finally, in fig. 11, we also present the output profile for a much longer

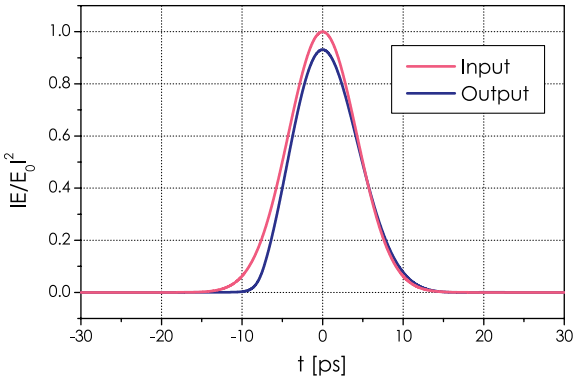


Fig. 11: (Colour on-line) Temporal profile comparison between the input $|E_{\rm in}/E_0|^2$ and the output $|E_{\rm out}/E_0|^2$ pulses in the dynamic case for a storing duration $\Delta t = 43.5 t_{\rm pass} \approx 1\,$ns.

storing duration $\Delta t = 43.5 t_{\rm pass} \approx 1\,$ns which is very similar to those presented in fig. 9. This last result shows that in our approach it is possible to reach a very high FD without pulse distortion in really short resonant photonic structures. In the chosen example, the FD is about 100. In this paper, we present the results for three particular values of $\Delta t$: $4.04 t_{\rm pass}$ in fig. 10, $8.1 t_{\rm pass}$ in fig. 9, and $43.5 t_{\rm pass}$ in fig. 11, but it is possible in theory with the same structure to discretely tune the storing duration. This is obtained by changing the loss/gain modulation duration by step of about $t_{\rm pass}$ from 0 to an arbitrary high value without pulse deformation.

**Discussion.** – In the simulations, we did not take into account the noise induced by the spontaneous emission in the second resonator. For small gain values and not too long storing durations this effect is not limiting [21,24,30], but for longer storing durations it would be mandatory to take it into consideration [30]. The assumed values of absorption and gain are consistent with III-V semiconductor devices [12,22]. It must be noted that another limiting parameter would be the speed of the loss/gain modulation which must be compatible with the pulse duration to store. In this work, the modulation speeds are consistent with loss switch based on the Stark effect [12] and the gain recovery time measurement in InAs/InGaAsP quantum dot amplifiers [31]. Still, in the case of III-V semiconductors, the material GVD around $1\,{\rm ps}^2/{\rm m}$ is negligible for 10 ps pulses [32,33]. The GVD induced by gain dispersion [32,34] can be evaluated about $60\,{\rm ps}^2/{\rm m}$ using a gain of $10\,{\rm cm}^{-1}$ and the parameters given in ref. [32] for semiconductor amplifiers. This gives a dispersion length of 60 cm, and thus a maximal storing duration of 5 ns assuming a pulse propagation velocity equal to $c/n$. Finally, the refractive index change due to gain modulation has not been taken into account. This phenomenon could lead to wavelength conversion during the storing process [29]. The wavelength conversion occurring during the storing process might be compensated by the wavelength conversion during the release process.

In a future more precise modeling of the process, this effect would have to be taken into account.

**Conclusion.** – We have theoretically shown a light-stopping process using a very compact sequence of microresonators relying on the dynamic modulation of optical losses and gain. This could not only be used as a very integrated all-optical discretely tunable buffer, but it could also be potentially used for reconfigurable dispersion compensation applications or nonlinear optics with low optical power. The simulations show that an implementation of the process in III-V semiconductor devices is compatible with 10 ps long pulses.

* * *

This work was partially backed by the French Agence Nationale de la Recherche through the project $O^2E$ (NT05-3-45032). The author acknowledges helpful discussions with P. Féron, G. Girault, A. Ricou, and V. Roncin.

REFERENCES

[1] Liu C., Dutton Z., Behroozi C. H. and Hau L. V., *Nature*, **409** (2001) 490.
[2] Phillips D. F., Fleischhauer A., Mair A., Walsworth R. L. and Lukin M. D., *Phys. Rev. Lett.*, **86** (2001) 783.
[3] Xia F., Sekaric L. and Vlasov Y., *Nat. Photon.*, **1** (2007) 65.
[4] Lenz G., Eggleton B. J., Madsen C. K. and Slusher R. E., *IEEE J. Quantum Electron.*, **37** (2001) 525.
[5] Khurgin J. B., *Opt. Lett.*, **30** (2005) 513.
[6] Mario L. Y. and Chin M. K., *Opt. Express*, **16** (2008) 1796.
[7] Baba T., *Nat. Photon.*, **2** (2008) 465.
[8] Bret B. P. J., Sonnemans T. L. and Hijmans T. W., *Phys. Rev. A*, **68** (2003) 023807.
[9] Yanik M. F. and Fan S., *Phys. Rev. Lett.*, **92** (2004) 083901.
[10] Yang Z. S., Kwong N. H., Binder R. and Smirl A. L., *Opt. Lett.*, **30** (2005) 2790.
[11] Khurgin J. B., *Phys. Rev. A*, **72** (2005) 023810.
[12] Sandhu S., Povinelli M. L. and Fan S., *Opt. Lett.*, **32** (2007) 3333.
[13] Longhi S., *Phys. Rev. E*, **75** (2007) 026606.
[14] Tanaka Y., Upham J., Nagashima T., Sugiya T., Asano T. and Noda S., *Nat. Mater.*, **6** (2007) 862.
[15] Xu Q., Dong P. and Lipson M., *Nat. Phys.*, **3** (2007) 406.
[16] Xiao J. J. and Yu K. W., *Opt. Commun.*, **281** (2008) 4023.
[17] Lin Q., Johnson T. J., Michael C. P. and Painter O., *Opt. Express*, **16** (2008) 14801.
[18] Yanik M. F. and Fan S., *Phys. Rev. A*, **71** (2005) 013803.
[19] Sandhu S., Povinelli M. L., Yanik M. F. and Fan S., *Opt. Lett.*, **31** (2006) 1985.
[20] Minin S., Fisher M. R. and Chuang S. L., *Appl. Phys. Lett.*, **78** (2004) 3238.
[21] Scheuer J., *EPL*, **77** (2007) 44004.
[22] Poon J. K. S., Zhu L., Choi J. M., Derose G. A., Scherer A. and Yariv A., *J. Opt. Soc. Am. B*, **24** (2007) 2389.
[23] Riyopoulos S., *Phys. Rev. A*, **75** (2007) 013801.
[24] Dumeige Y., Nguyen T. K. N., Ghisa L., Trebaol S. and Féron P., *Phys. Rev. A*, **78** (2008) 013818.
[25] Smith D. D., Chang H., Fuller K. A., Rosenberger A. T. and Boyd R. W., *Phys. Rev. A*, **69** (2004) 063804.
[26] Van V., Ding T.-N., Herman W. N. and Ho P.-T., *IEEE Photon. Technol. Lett.*, **20** (2008) 997.
[27] Pereira S., Chak P. and Sipe J. E., *J. Opt. Soc. Am. B*, **19** (2002) 2191.
[28] Pereira S., Chak P., Sipe J. E., Tkeshelashvili L. and Busch K., *Photon. Nanostruct. Fundam. Appl.*, **2** (2004) 181.
[29] Notomi M. and Mitsugi S., *Phys. Rev. A*, **73** (2006) 051803.
[30] Khurgin J. B., *Opt. Lett.*, **32** (2007) 163.
[31] Zilkie A. J., Meier J., Smith P. W. E., Mojahedi M., Aitchison J. S., Poole P. J., Allen C. N., Barrios P. and Poitras D., *Opt. Express*, **14** (2006) 11453.
[32] Agrawal G. P., *IEEE J. Quantum Electron.*, **27** (1991) 1843.
[33] Modotto D., Mondia J. P., Linden S., Tan H. W., Morandotti R., Kleckner T. C., Locatelli A., De Angelis C., van Driel H. M., Stanley C. R. and Aitchison J. S., *Opt. Commun.*, **249** (2005) 201.
[34] Gordon R., Heberle A. P. and Cleaver J. R. A., *J. Opt. Soc. Am. B*, **21** (2004) 29.